Vector Imitation Model of Semiflexible Polymers: Application to Polymer Adsorbed on a Spherical Particle

Iliya Kusner and Simcha Srebnik*

Department of Chemical Engineering, Technion−Israel Institute of Technology, Haifa, Israel 32000

Received November 27, 2006; Revised Manuscript Received April 10, 2007

ABSTRACT: We introduce a new type of model that imitates polymer behavior of semiflexible polymers. In this model, the energy and entropy contributions to the free energy are treated as forces that act on the individual monomers, and thus guide the "movement" or "growth" of the chain. The model falls at the interface between theory and simulation, allowing statistical prediction of polymer conformational behavior of long polymer chains at a small computational cost. Results are compared with theoretical predictions by Spakowitz and Wang (SW) (*Phys. Rev. Lett.* **2003**, *91*, 166102) of the behavior of semiflexbile chain confined to the surface of a sphere and our own Monte Carlo simulations. The SW and Monte Carlo results are reproduced with the imitation model with surprising accuracy. The simple nature of the imitation model allows us to carry out calculations for very long chains, with which we show that the surface coverage of the sphere is a non-monotonic function of persistence length for a given fixed chain length, distinguishing between random, wrapping, and ring conformations.

1. Introduction

The large number of degrees of freedom of even a single polymer chain presents a formidable problem for all but the simplest case of the ideal Gaussian chain. Though it is straightforward to write an expression for the partition function and associated thermodynamic averages for a given model of a polymer chain, including nonbonded interactions between distant segments, other chains, or an external potential, it is in general not feasible to carry out exact calculations analytically.

For the semiflexible chain, the Krakty−Porod[2] wormlike chain model provided the first rigorous analysis, with an analytic expression for the end-to-end distance as a function of chain persistence length. However, the inability to calculate the end-to-end distance distribution from the Kratky−Porod model meant that direct comparison with experiments was not possible.[3,4] Kholodenko[5] introduced the Dirac chain model, which provides an analytical expression for the chain propagator. However, while the Dirac model accurately predicts chain behavior at the flexible and rigid limits, it is not accurate in the semiflexible regime.[6] Wilhelm and Frey arrived at an approximate analytical expression for the end-to-end distance distribution of semiflexible chains, which showed good agreement with MC simulations for the stiffer chains but poorly predicted the end-to-end distance distribution at the flexible regime.[7]

Polymer theory appears specifically underdeveloped for problems involving semiflexible chains in confined environments because of finite dimensionality. Moreover, there is no consistent theory at the present time for the behavior of confined semiflexible macromolecules, such as that developed for flexible chains.[8−10] Using the Kratky−Porod wormlike chain model,[2] Yamakawa and Stockmayer[11] were the first to address the way that degrees of freedom may be lost when a stiff chain is coiled tightly into a circle of radius less than its persistence length, λ_p. Similarly, in narrow pores, a macromolecule is heavily deformed, and its behavior is no longer universal and becomes dependent both on the conformational properties of the macromolecule (its topology, rigidity, excluded volume effects) and on the pore form, i.e., on the nature of boundary constraints. More recently, Kholodenko et al.[12] extended the Dirac chain model to treat the problem of semiflexible chains confined between adsorbing flat parallel plates and similarly showed that chain dimensions of stiff chains are determined by the confining geometry. However, the complexity of these theories renders their extension to other geometries and physically relevant problems difficult.

In this communication, we introduce an imitation model of semiflexible chains that is based on thermodynamic considerations, and which provides a simple means for qualitatively describing polymer behavior. In the model, the competition between energy and entropy is interpreted as separate "energetic" and "entropic" forces that determine the location of the next monomer in a growing chain. In its basic form, the model reduces to simulating ideal random walk behavior. Our method can be modified to include various complications in the dilute-solution regime, such as irregular confining geometries or self-avoidance,[13] which are difficult to incorporate into existing theories.

We apply the concept to a semiflexible chain and then treat the problem of a semiflexible chain confined to the surface of a sphere. We compare the results with the theoretical predictions by Spakowitz and Wang[1] (SW) and Monte Carlo (MC) simulations, which provide us with an instrument to check the SW theory. We find that the SW model is very accurate in predicting the behavior of semiflexible chains confined to the surface of a sphere, and agreement with the MC results is excellent. In addition, we show that the imitation method confirms the results of ref 1 and sheds additional insight into the problem of very long chains.

The remainder of the manuscript is organized as follows. In section 2, we present the vector imitation model (VIM), detailing its thermodynamic basis and its basic construction for a semiflexible polymer chain. In section 3, we briefly describe the Monte Carlo simulation used to test the model. In section 4, we present and discuss our results, and compare them with the SW model. We offer concluding remarks in section 5.

* Corresponding author. E-mail: simchas@technion.ac.il.

10.1021/ma062721+ CCC: $37.00
Published on Web 07/18/2007

2. Vector Imitation Model

Statistical thermodynamics in principle provides us tools for calculating the partition function and the corresponding thermodynamic properties of any given system. However, apart from very simple cases, the free energy of a given system cannot be calculated exactly. Deviation from ideal behavior cannot in general be captured theoretically, and molecular simulation often provides the only available predictive tool. Statistically, configurations that lead to large energy penalities have a much lower chance of occurring, their probability being given by their Boltzmann weight. The Metropolis MC method[14] provides a means to sample the relevant configurations, and thus obtain a very good approximation of thermodynamics properties as averages over a large number of statistically relevant configurations.

The general purpose of the imitation model is to reproduce a given process by an equivalent, though much simpler, process that is easier to analyze. The imitation model reproduces events, their consequence, and the synchronization between them. That is, a particular polymer conformation (consequence) is governed by (synchronized with) the presence of other events (e.g., surface or another polymer). The presented imitation model is implemented as a directed growth process of a freely jointed chain and applied to the problem of a semiflexible chain confined to the surface of a sphere.

Thermodynamic equilibrium properties are determined by the competition between the entropic drive to sample a large number of conformations and the internal and external energetic constraints of the system. As an example, we consider a semiflexible polymer. In this case, we can view the energy as a force drawing the polymer toward a linear conformation, while entropy draws the polymer to sample a large number of different and random conformations. In the vector imitation model (VIM), we account for these effects by introducing "energy" and "entropy" vectors acting on each polymer segment; the sum of these vectors determines possible conformations of the polymer. For the ideal case of a Gaussian chain, statistical properties are derived from random walk statistics, and the chain conformation behavior, apart for the constraint of chain connectivity, is purely entropic. Thus, to obtain average chain dimensions (e.g., end-to-end distance, R) of a chain of contour length $L = Nl$ (where N is the number of chain segments and l is the effective segment size), one needs to carry out simple Gaussian integrals to obtain exact results. Approximate results can be obtained numerically by averaging properties over a large sample of random walks.

Ideal chain statistics can be generated from a vector model where a sample chain conformation is obtained from successive addition of random vectors $\mathbf{s}_i$ of length l,[15]

$$\mathbf{R}_{\text{ideal}} = \sum_{i=1}^{N} \mathbf{s}_i \tag{1}$$

where $|\mathbf{s}_i| = |\mathbf{r}_{i+1} - \mathbf{r}_i| = l$ is the bond vector connecting monomer i located at $\mathbf{r}_i$ and monomer $i - 1$ located at $\mathbf{r}_{i-1}$. Deviations from ideal behavior result from additional constraints such that equilibrium behavior is no longer determined solely by entropic driving force. Specifically, for semiflexible chains, the energy penalty of bending has the effect of limiting the conformational space available for the polymer and drives toward low entropy linear conformations ($R \sim L$), while the entropic drive is toward Gaussian dimension ($R \sim L^{1/2}$). The chain internal energy is determined by the bending potential characterizing the stiffness of the chain, $u_b(\theta)$, summed over all bond angles, where θ is the bond angle depicted in Figure 1. Similar to the calculation of the random-walk chain in eq 1, we can imagine as a simplistic model of a semiflexible chain the addition of another vector, **e**, which directs the placement of each chain segment. As a first approximation, the direction of **e** is taken to be dependent only on the location of the current and previous chain segments, and whose magnitude depends on chain stiffness. In the absence of entropic effects, we would obtain a rigid rod conformation with zero bending angles given by

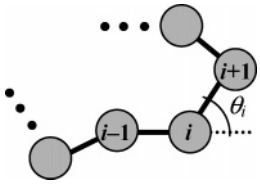

Figure 1. Schematic illustration of a polymer chain with bond angle θ_i.

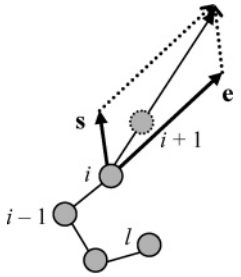

Figure 2. Schematic depiction of the vector imitation model. Position of monomer $i + 1$ is obtained from the sum of two vectors, **e** and **s**, acting on monomer i. **e** points in the direction of bond vector $(\mathbf{r}_i - \mathbf{r}_{i-1})$ and the direction of **s** is random.

$$\mathbf{R}_{\text{rigid}} = \sum_{i=1}^{N} \frac{\mathbf{e}_i}{|\mathbf{e}_i|} l \tag{2}$$

Combining the "entropy" and "energy" vectors, we get a chain movement or growth process where the position of the next monomer depends only on the location of the two previous monomers. If we neglect nonbonded interactions, then the vector **e** has constant magnitude, a, that depends on bending stiffness. Thus, we can write

$$\mathbf{r}_{i+1} = \mathbf{r}_i + \frac{\mathbf{s}_i + \mathbf{e}_i}{|\mathbf{s}_i + \mathbf{e}_i|} l = \mathbf{r}_i + \frac{\mathbf{u}_{\mathbf{s},i} + a\mathbf{u}_{\mathbf{e},i}}{|\mathbf{u}_{\mathbf{s},i} + a\mathbf{u}_{\mathbf{e},i}|} l \tag{3}$$

where $\mathbf{u}_\mathbf{s}$ is a unit vector that points in a random direction and $\mathbf{u}_\mathbf{e} = (\mathbf{r}_i - \mathbf{r}_{i-1})/l$ is a unit vector that extends in the direction of the bond vector connecting monomers i and $i - 1$. Normalization ensures that the distance between monomers i and $i + 1$ equals l. Thus, we have one independent parameter, which we later relate to persistence length. Clearly, when $a = 0$, we obtain random walk statistics, and when $a \gg 0$, we obtain a rigid rod. The generation of a chain conformation using the imitation model is illustrated in Figure 2.

Because of the probabilistic nature of the "entropy" vector, results are obtained as averages over a large number of experiments. Since the direct calculation of bending energy is not required in this model, simulations are carried out very quickly. The principles of constructing such an imitation model allow us to easily account for other factors, such as other interacting bodies, different geometries, long-range interactions, heteropolymers, and branched polymers.

We examine the model predictions against the theory presented by Spakowitz and Wang[1] for the confinement of a

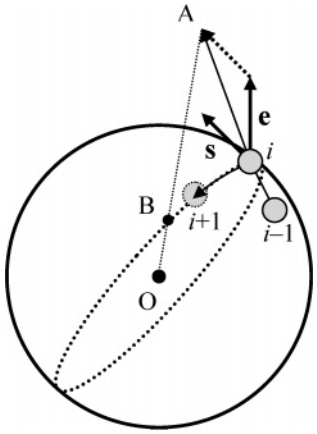

Figure 3. Depiction of the vector imitation model on a spherical surface. Position of bead $i + 1$ is determined from a point along the path of a great circle connecting monomer i and the intersection of line OA with the surface of the sphere.

semiflexible chain to the surface of a sphere and our own MC simulation of semiflexible chains (described in section 3). The application of the vector model to a spherical surface is shown in Figure 3. In this case, it is assumed the vectors **e** and **s** act as before, with the additional constraint that the monomers lie on the surface of the sphere. This is accomplished by finding the intersection of the position of monomer $i + 1$, as determined by vectors **e** and **s** in space (point A in Figure 3), and projecting it on the surface of the sphere. In other words, the final position of monomer $i + 1$ is determined by the path along the great circle connecting monomer i and the intersection (point B) of the sphere surface with line AO connecting point A with the center of the sphere O, a distance l from monomer i.

3. Monte Carlo Simulation

We simulated the behavior of a single semiflexible polymer chain using off-lattice Monte Carlo method. The polymer chain is modeled as a pearl necklace made up of N identical penetrable beads of diameter σ and bond length $l = 1\sigma$. A harmonic bending energy potential was used to account for chain stiffness,[16]

$$U = \kappa \sum_{i=3}^{N} (1 - \cos \theta_i)^2 \tag{4}$$

where θ_i is the bond angle calculated from $\cos \theta_i = \{(\mathbf{b}_{i-1} \cdot \mathbf{b}_i)\}/\{|\mathbf{b}_{i-1} \cdot \mathbf{b}_i|\}$ (Figure 1), and $\mathbf{b}_i = \mathbf{r}_i - \mathbf{r}_{i-1}$. κ provides a measure of bending stiffness of the polymer. According to eq 4, the potential energy of the chain is at a minimum for a rigid rod conformation.

The initial polymer configuration is obtained by growing the chain one monomer at a time in a random direction, disregarding the bond energy. Equilibration and sampling of the polymer configurational space is achieved using a combination of reptation and kink-jump moves.[17] Each reptation move constitutes the displacement of one of the chain ends by a distance l in a random direction, drawing the remaining units along in a snake-like movement. A kink-jump move is the rotation of any chain unit, except end units, by a random angle around a virtual bond connecting its two adjacent units. The moves are accepted according to a standard Metropolis algorithm,[14] with the acceptance probability given by

$$p = \min [\exp(-(U_{\text{new}} - U_{\text{old}})/kT), 1] \tag{5}$$

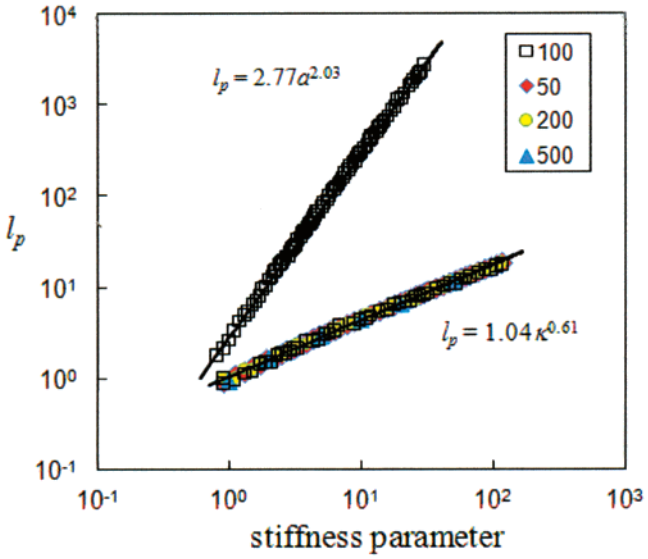

Figure 4. Persistence length as a function of stiffness parameters, a and κ, calculated from the bond angle correlation function, for different chain lengths.

where the subscripts stand for the new and old configurations. Equilibration required on average 10^4-10^5 MC simulation steps, where each MC step constitutes N trial moves. To ensure equilibration, 10^6 MC steps were performed prior to calculating average properties. Averages were calculated over values taken every 10^2 MC steps for an additional 5×10^5 MC steps. Simulations were carried for various values of N and κ in order to relate the bond stiffness parameter to persistence length.

The same algorithm was used for a chain confined to the surface of a sphere. However, since on a sphere, a kink-jump move about bead i defines a specific location on the surface, it was found that the acceptance rate of kink-jump moves is very low beyond the initial period of chain relaxation for the case of semiflexible chains. Thus, only reptation moves were used in equilibration and data collection, where each move constitutes displacement of one of the chain ends to a random location on a small circle defined by the confining sphere and a sphere with radius l centered around bead i.

4. Results and Discussion

4.1. 3D Space. The stiffness parameter, a appearing in eq 1, and the bending stiffness parameter, κ of eq 4, can be related to polymer persistence length l_p through the bond-angle correlation function (BAC), defined according to ref[18]

$$\text{BAC}(x) = \left\langle \frac{\mathbf{s}_i \mathbf{s}_{i+x}}{|\mathbf{s}_i||\mathbf{s}_{i+x}|} \right\rangle \sim \exp(xl/l_p) \tag{6}$$

where the average is carried out over monomers separated by x units along the contour of the chain and over all conformations. BAC(x) decays exponentially, and the persistence length is defined as the decay length, l_p. Figure 4 shows our results for l_p as a function of a and κ obtained from the imitation model (for $N = 100$) and from the MC simulation (for $N = 50$, 100, 200, 500), respectively. The relations are well fitted by power law relations $l_p \sim \kappa^{0.61}$ and $l_p \sim a^{2.0}$ for $\kappa > 1$ and $a > 1$, respectively, and are not sensitive to chain length. These empirical relations are used to quantitatively compare the results of the model and simulation, and analyze the results in terms of the physical parameter, l_p.

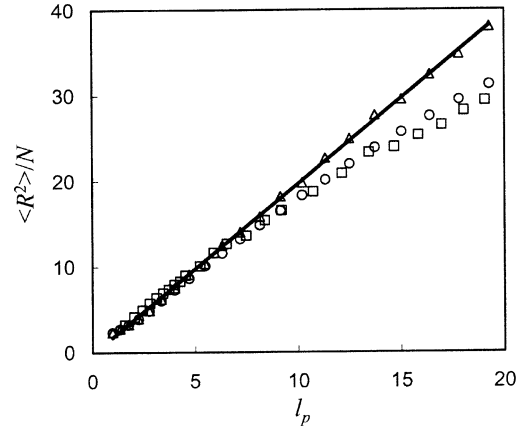

Figure 5. End-to-end distance as a function of persistence length for semiflexible chains in 3-dimensional space as predicted by the vector imitation model averaged over 5E3 conformations for $N = 500$ (triangles) and averaged over 1E6 conformations for $N = 100$ (circles), and MC simulation averaged over 5E3 conformations for $N = 100$ (squares).

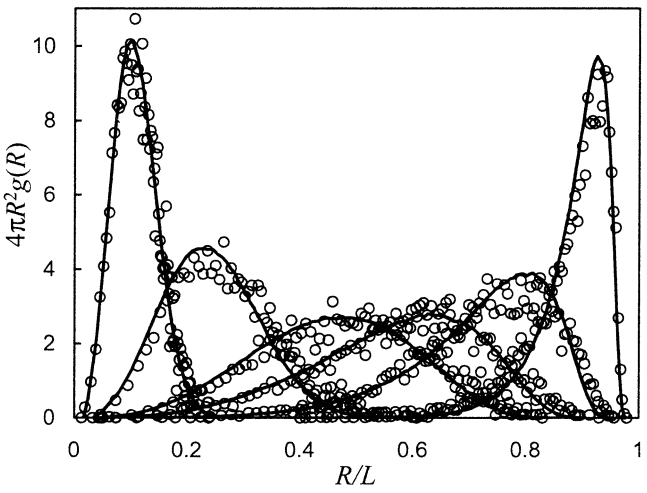

Figure 6. End-to-end distance distribution as obtained from the vector imitation model averaged over 10^6 conformations (solid curves) and MC simulation averaged over $5{\cdot}10^3$ conformations (symbols) from left to right for $L/l_p = 100$, 40, 10, 5, 2, and 0.5 (where $L = Nl$).

The squared end-to-end distance of a semiflexible polymer chain is known to grow linearly with the persistence length. The imitation model correctly predicts the linear dependence of the squared end-to-end distance with persistence length, as seen in Figure 5. Deviation from linear behavior at large l_p, predicted by the model and MC simulation is due to the short chains sampled; however, the quantitative agreement with MC simulation is excellent.

To further evaluate our model, we calculated the end-to-end distance distribution, $g(R)$, for the entire spectrum of persistence lengths, from flexible to rigid chains. In Figure 6, we compare the end-to-end distance distributions of the configurations sampled by the simulation and model for several values of persistence length. The agreement between the imitation model and simulation is excellent, with only slight deviation at large values of R for the rigid chains. To, our knowledge, this is the first model that accurately captures the conformational statistics of semiflexible chains for the entire range of bond bending stiffness.

4.2. Sphere. Next, we applied the model to the problem of a polymer chain confined to the surface of a sphere. An analytical solution was recently offered by Spakowitz and Wang (SW).[1] They determined a critical ratio of sphere radius to chain

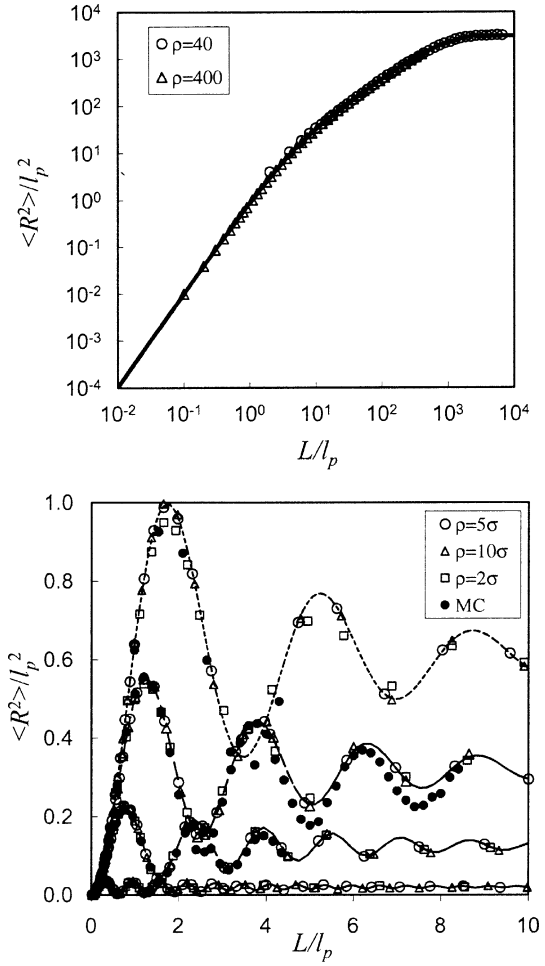

Figure 7. Average square end-to-end distance vs polymer chain length as predicted by SW theory (lines), MC simulation (filled symbols) and imitation model (open symbols) for the following ρ/l_p ratios: (a) $\rho/l_p = 40$ and (b) $\rho/l_p = 1/10$ (solid line), $\rho/l_p = 1/4$ (dashed line), $\rho/l_p = 2/5$ (dash-dotted line), and $\rho/l_p = 11/20$ (dotted line). MC simulations is shown for $\rho = 5\sigma$; imitation model is shown for $\rho = 2\sigma$ (squares), $\rho = 5\sigma$ (circles), and $\rho = 10\sigma$ (triangles).

persistence length ($\rho/l_p = 4$) below which oscillatory behavior of ρ/l_p as a function of chain length was observed. Such behavior was attributed to orbital wrapping of the polymer around the sphere. Comparison between SW theory, MC simulations, and our model is shown in Figure 7 for various ρ/l_p ratios. Excellent agreement between the model, simulations, and theory is observed for the entire range of parameter values. It is important to note that no fitting parameters were used in either the simulation nor the model; the value of l_p is obtained from fitting to eq 6 and is independent of the method. The efficacy of the imitation model became especially apparent in generating these plots since it allowed us to obtain results for long chains ($\sim 10^4$ monomers) averaged over a large number of conformations quickly and with very modest computational resources.

To gain further insight into the problem of polymer confined to the surface of a sphere, we calculated the average local density of the polymer on the sphere, $d = N/A$, where A is a unit surface area. In Figure 8, we plot the reduced density, $\delta = (d/d_0 - 1)$, as a function of chain length, where d_0 is the average local density of a Gaussian chain of chain length $L = N\sigma$. As expected, for large L, the semiflexible chain approaches the Gaussian limiting density ($\delta \rightarrow 0$). For $a \leq 10$ ($l_p \leq 300$), the semiflexible chain covers the surface more efficiently then the Gaussian chain, since $\delta < 0$; these curves go through a minimum indicative of chain length beyond which even coverage of the

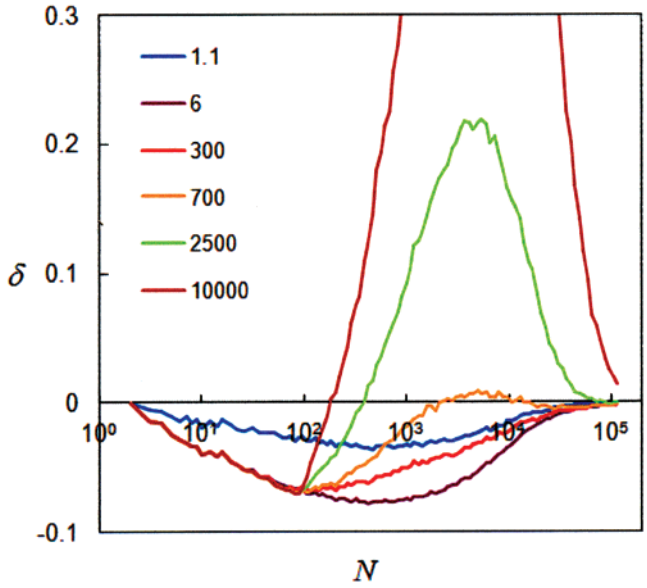

Figure 8. VIM results for the reduced segment density, δ, as a function of chain length for $\rho = 5\sigma$, and different values of l_p.

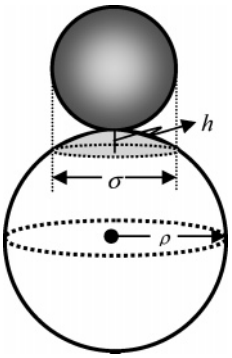

Figure 9. Schematic depiction of the surface area covered by a monomer of size σ on a sphere of radius ρ.

surface has been achieved and chain overlap occurs. However, the rigid chain displays qualitatively different behavior, with δ taking values greater than zero for a finite range of N. For short rigid chains, $\delta < 0$ simply because the no segment overlap occurs as opposed to the Gaussian chain. Once complete encircling of the sphere is achieved, the density grows (rapidly for the rigid rod limit) as the chain proceeds to wrap the sphere in essentially the same course. Eventually, even the rigid chain approaches the density of a Gaussin chain at chain lengths of the order of $10l_p$, as is expected from the diffusive nature of the model.

The fractional surface area of the sphere covered by the polymer chain with bead size $\sigma = l$ was also studied. A simple calculation would involve projection of the sphere and polymer on a fine grid and counting the fraction of surface sites that the polymer occupies. However, the accuracy of the results is limited by computational resources (i.e., the number of grid sites per σ), especially for $\rho > 2\sigma$. Thus, the surface area covered by the polymer was approximated as follows. A single monomer occupies an area, SA_m, that corresponds to the projection of a sphere of diameter σ on a sphere of diameter ρ, as illustrated in Figure 9, given by

$$SA_m = 2\pi\rho h = 2\pi\rho^2(1 - \sqrt{1 - (\sigma/2\rho)^2}) \qquad (7)$$

To account for the surface area covered by overlapping monomers, we assumed that the projected surface area on the sphere is proportional to the distance between the centers of the overlapping monomers, so that the total surface area covered by a chain made up of N monomers is approximated by

$$SA \approx N \cdot SA_m - \sum_{i=2}^{N} \sum_{j<i} SA_1 (1 - f_i)|\mathbf{r}_i - \mathbf{r}_j|/l \qquad (8)$$

where f_i is the fraction of monomer i that overlaps with all other monomers.

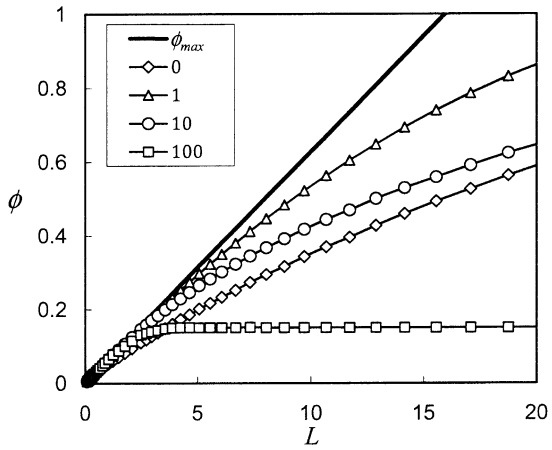

Figure 10. Fractional surface coverage as a function of chain length for various values of stiffness parameter, a. Solid line corresponds to maximum surface coverage possible for a given chain length on sphere with radius $\rho = 5\sigma$.

The fractional surface coverage, $\phi = SA/4\pi\rho^2$ as a function of $L\sigma/\rho^2$ is plotted in Figure 10 for various values of l_p, and it is compared with the maximum possible surface coverage. Similar to Figure 8, it is seen that semiflexible chains achieve full surface coverage at a rate that depends on chain stiffness. Stiff chains reach a plateau value of surface coverage that corresponds to the surface area of a ring of monomers encompassing the sphere around its equator; i.e., very stiff chains will cover only a very small fraction of the surface at finite chain lengths. Clearly, the latter phenomenon is a manifestation of the ideal model and will not be observed with the more realistic model of excluded volume chains. Further, the surface area covered by a chain is nonmonotonic with respect to persistence length. This is more clearly seen in Figure 11, where we plot the normalized chain length required to achieve full coverage $\lambda = L\sigma/\rho^2|_{\phi=1}$ (Figure 11a), the surface coverage for a fixed chain length (Figure 11b), and the maximum surface coverage ϕ_∞ observed at infinite chain length (Figure 11c), as a function of chain stiffness. The slight initial decrease in λ seen at $l_p/\rho < 1$ (corresponding to chain persistence lengths of the order of unity), is explained by the faster "diffusion" over the surface of the sphere achieved by the somewhat less flexible chain. The semiflexible chain, with l_p/ρ in the range 1−10, achieves efficient coverage of the sphere surface with a minimal chain length through orbiting around the sphere in a wrapping like manner (depicted in Figure 12). With increasing chain stiffness, increasingly longer lengths are required to fully wrap the sphere as smaller conformational fluctuations are allowed, as clearly observed in Figure 11b. The very stiff chain requires infinite length to achieve full coverage as conformational fluctuations lead to slight departures from a perfect ring. The attained sphere surface coverage at infinite chain length, ϕ_∞, decreases linearly with chain stiffness beyond a critical value of chain stiffness, a_c, as seen in Figure 11c. The linear dependence is expected since the magnitude of the fluctuations from a perfectly circular path is proportional to a, by definition

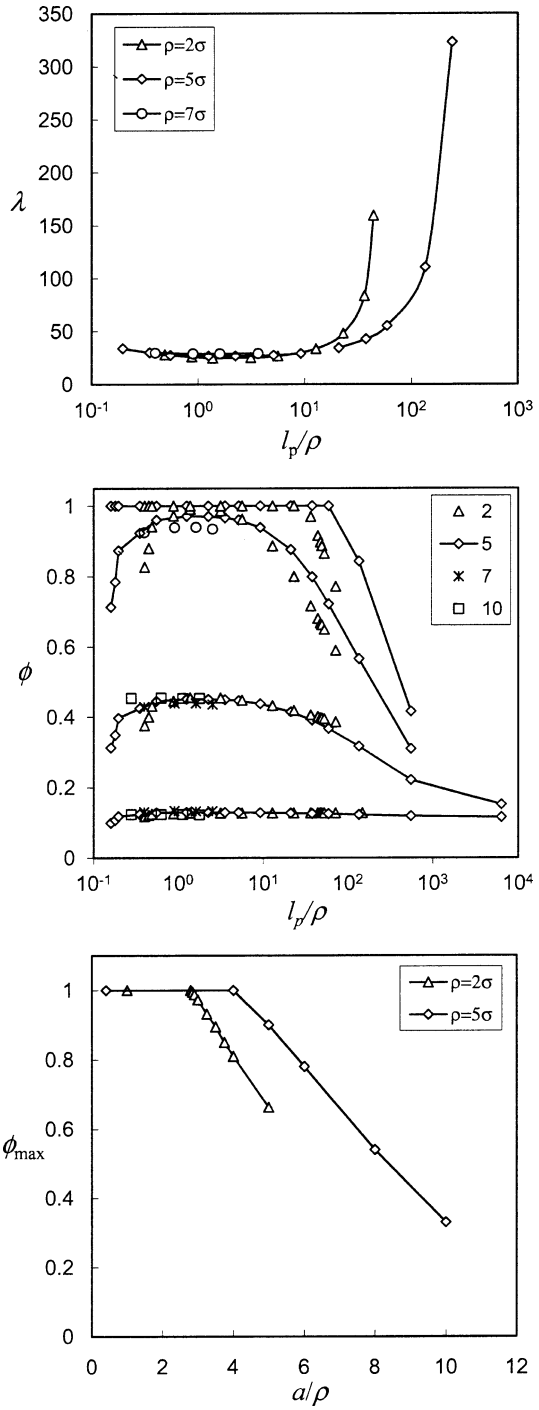

Figure 11. (a) Normalized chain length required to achieve full coverage of the sphere as a function of l_p/ρ, (b) fractional coverage of the sphere as a function of persistence length, and (c) surface coverage at infinite chain length for different sphere radii.

of the imitation model (eq 3). These three conformational phases are shown in Figure 12. A coil configuration at low l_p samples the surface of the sphere in a diffusive manner and does not efficiently cover the sphere surface (Figure 12a), while very stiff chains orbit the sphere around the equator (Figure 12c). Intermediate chain stiffness leads to efficient wrapping of the sphere due to sufficient conformational fluctuations away from the energetically favored ring conformations (Figure 12b). These three phases are analogous to the coil, helical, and linear conformations that were recently reported for semiflexible polymers confined the surface of a cylinder.[19]

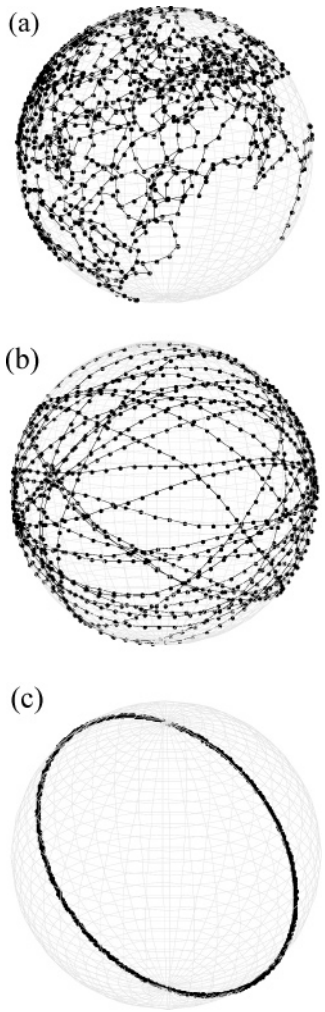

Figure 12. Sample chain conformations for polymer chain made up of $N = 1000$ monomers confined to a sphere with radius $\rho = 10\sigma$ for different values of l_p. (a) $l_p = 1\sigma$, coil conformation; (b) $l_p = 25\sigma$, wrapped conformation; (c) $l_p = 300\sigma$, ring conformation.

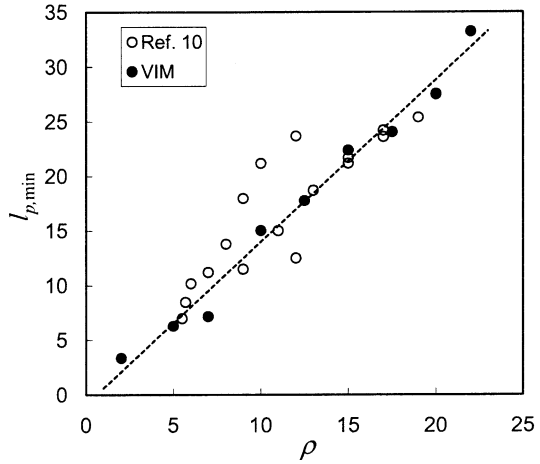

Figure 13. Persistence length for which minimum chain length is required to achieve full coverage (black circles) and characteristic persistence length for which helical conformations were observed in ref 16 (white circles) vs sphere radius.

Cerda et al.[16] carried out MC simulations of excluded volume chains confined near the surface of a sphere. They observed the formation of helical conformations beyond a limiting ratio of chain persistence length to sphere radius. Furthermore, a linear relationship was obtained between the critical persistence length and sphere radius. Figure 13 shows a plot of $l_{p,c}$, the

persistence length for which full coverage of the sphere is obtained at minimum chain length (from Figure 11a), as a function of ρ. The results are compared with those obtained in ref 16, where the same linear dependence was found between the critical persistence length beyond which helical conformations were observed. This critical persistence length indicates the onset of wrapping conformations, which shift to ring conformations with increasing chain stiffness. Both the wrapping and ring conformations observed in the VIM would lead to helical orbiting observed for excluded volume chains in ref.[16]

5. Concluding Remarks

We introduce the concept of imitation modeling to study polymer behavior. The model relies on the competing effect of energy and entropy, which pull the chain toward a linear conformation (for semiflexible chains) or a random coil conformation, respectively. Predictions of the imitation model were found to be in excellent agreement with MC simulation and theoretical calculations in the case of a semiflexbile chain confined to the surface of a sphere (SW model). The end-to-end distance distributions were reproduced by the VIM for the entire range of persistence lengths studied. Because of the simplicity of the imitation model, we were able to simulate the thermodynamic behavior of very long ($N \sim 10^4$) chains, and thus distinguish between three conformation phases—random, wrapping, and ring conformations—that correspond to flexible, semiflexible, and stiff chains, respectively. When the persistence length is of the order of the size of a segment, the chain covers the surface of the sphere in a diffusive manner, leaving areas of the sphere exposed. Chains with moderate persistence lengths wrap the sphere in circular orbits that encompass the entire surface of the sphere. Very stiff chains form rings around the equator, leaving the majority of the sphere surface exposed. The basic principles on which the imitation model relies allows it to be easily extended to account for other phenomena, such as excluded volume, other intersegment or external interactions, and other geometries.

Acknowledgment. This work has been funded in part by the Israel Science Foundation.

References and Notes

(1) Spakowitz, A. J.; Wang, Z. G. *Phys. Rev. Lett.* **2003**, *91*, 166102.
(2) Kratky, O.; Porod, G. *Pays-Bas* **1949**, *68*, 1106.
(3) Kholodenko, A. L. *J. Chem. Soc., Faraday Trans.* **1995**, *91*, 2473−2482.
(4) Kholodenko, A.; Ballauff, M.; Granados, M. A. *Physica A* **1998**, *260*, 267−293.
(5) Kholodenko, A. *Phys. Lett. A* **1989**, *141*, 351.
(6) Potschke, D.; Hickl, P.; Ballauff, M.; Astrand, P. O.; Pedersen, J. S. *Macromol. Theory Simul.* **2000**, *9*, 345−353.
(7) Wilhelm, J.; Frey, E. *Phys. Rev. Lett.* **1996**, *77*, 2581−2584.
(8) Casassa, E. F. *J. Polym. Sci. Part B: Polym. Lett.* **1967**, *5*, 773-&.
(9) Casassa, E. F. *Macromolecules* **1976**, *9*, 182−185.
(10) Casassa, E. F.; Tagami, Y. *Macromolecules* **1969**, *2*, 14−26.
(11) Yamakawa, H.; Stockmayer, W. H. *J. Chem. Phys.* **1972**, *57*, 2843−2854.
(12) Kholodenko, A. L.; Bearden, D. W.; Douglas, J. F. *Phys. Rev. E* **1994**, *49*, 2206−2224.
(13) Excluded volume can be introduced into the imitation model in the conventional way of including memory, but with the introduction of a nonconventional imitative model to treat the overlap when it is encountered, such as reflective conditions on the vector sum.
(14) Metropolis, N.; Rosenbluth, A. W.; Rosenbluth, M. N.; Teller, A. H.; Teller, E. *J. Chem. Phys.* **1953**, *21*, 1087−1092.
(15) de Gennes, P. G. *Scaling concepts in polymer physics*; Cornell University Press: Ithaca, NY, 1979.
(16) Cerda, J. J.; Sintes, T.; Chakrabarti, A. *Macromolecules* **2005**, *38*, 1469−1477.
(17) Baschnagel, J.; Wittmer, J. P.; Meyer, H. In *Computational Soft Matter: From Synthetic Polymers to Proteins*; Attig, N., Binder, K., Grubmuller, H., Kremer, K., Eds.; John von Neumann Institute for Computing: Julich, Germany, 2004; Vol. 23, pp 83−140.
(18) Micka, U.; Kremer, K. *J. Phys.-Condens. Matter* **1996**, *8*, 9463−9470.
(19) Kusner, I.; Srebnik, S. *Chem. Phys. Lett.* **2006**, *430*, 84−88.

MA062721+